Molecular Genetics and Metabolism Reports 21 (2019) 100512

Contents lists available at ScienceDirect

Molecular Genetics and Metabolism Reports

journal homepage: www.elsevier.com/locate/ymgmr

The CRISPR-Cas9 crADSL HeLa transcriptome: A first step in establishing a model for ADSL deficiency and SAICAR accumulation

Randall C. Mazzarino[a,b,c,d], Veronika Baresova[e], Marie Zikánová[e], Nathan Duval[a,b,c], Terry G. Wilkinson II[a,b,c], David Patterson[a,b,c,d], Guido N. Vacano[a,b,c,*]

[a] Knoebel Institute for Healthy Aging, University of Denver, 2155 E. Wesley Avenue, Denver, CO 80210, USA
[b] Eleanor Roosevelt Institute, University of Denver, Denver, CO 80210, USA
[c] Department of Biological Sciences, University of Denver, Denver, CO 80210, USA
[d] Molecular and Cellular Biophysics Program, University of Denver, Denver, CO 80210, USA
[e] Research Unit for Rare Diseases, Department of Pediatrics and Adolescent Medicine, First Faculty of Medicine, Charles University and General University Hospital in Prague, Prague, Czech Republic

ARTICLE INFO

Keywords:
RNA-seq
Purine synthesis
Transcriptome
Adenylosuccinate lyase

ABSTRACT

Adenylosuccinate lyase (ADSL) catalyzes two steps in de novo purine synthesis (DNPS). Mutations in ADSL can result in inborn errors of metabolism characterized by developmental delay and disorder phenotypes, with no effective treatment options. Recently, SAICAR, a metabolic substrate of ADSL, has been found to have alternative roles in the cell, complicating the role of ADSL. crADSL, a CRISPR KO of ADSL in HeLa cells, was constructed to investigate DNPS and ADSL in a human cell line. Here we employ this cell line in an RNA-seq analysis to initially investigate the effect of DNPS and ADSL deficiency on the transcriptome as a first step in establishing a cellular model of ADSL deficiency. We report transcriptome changes in genes relevant to development, vascular development, muscle, and cancer biology, which provide interesting avenues for future research.

1. Introduction

Defects in de novo purine synthesis (DNPS) can cause inborn errors of metabolism. Of particular interest, adenylosuccinate lyase (ADSL) deficiency, an autosomal recessive inborn error of metabolism, has been observed in approximately 80 individuals to date [1] and is typically diagnosed by SAICA-riboside accumulation in biofluids [2]. With advances in genomic sequencing and reduction in cost, it is likely that the number of diagnosed ADSL deficient patients will increase in the future. The phenotype of ADSL deficiency is variable and affects multiple systems, presenting as fatal neonatal, severe, or mild to moderate forms including features such as seizures, autistic traits, psychomotor retardation, respiratory failure, and microcephaly. This implies that there are significant alterations in gene expression in ADSL deficiency. The ADSL enzyme is a homotetramer and mutations in ADSL can result in altered tetramer stability or active site disruption resulting in reduced levels of enzyme activity [3]. In the most severe cases, enzyme activity may be reduced by as much as 75%.

DNPS is one of the most ancient biochemical pathways [4]. In mammalian DNPS, phosphoribosyl pyrophosphate (PRPP) is converted to inosine monophosphate (IMP) in ten enzymatic steps by six different enzymes. IMP is converted to either adenosine monophosphate (AMP) or guanosine monophosphate (GMP) via two additional enzymatic steps (Fig. 1). ADSL is a bifunctional homotetrameric enzyme that catalyzes the eighth step, forming aminoimidazole carboxamide ribonucleotide (AICAR) from phosphoribosylaminoimidazolesuccinocarboxamide (SAICAR). It is also responsible for the final step in the conversion of IMP to AMP, specifically cleaving succinyladenosine monophosphate (SAMP) into AMP (Fig. 1). ADSL is thought to be an enzyme with straightforward and defined functions, however recent evidence suggests a more complicated cellular role.

The DNPS intermediates and products have multiple functions

Abbreviations: adenosine monophosphate, (AMP); adenylosuccinate lyase, (ADSL); aminoimidazole carboxamide ribonucleotide, (AICAR); de novo purine synthesis, (DNPS); differentially expressed gene, (DEG); false discovery rate, (FDR); fetal calf macroserum, (FCM); fragments per kilobase of exon per million reads mapped, (FPKM); gene ontology, (GO); guanosine monophosphate, (GMP); minus adenine crADSL to minus adenine WT comparison, (MM); phosphoribosyl pyrophosphate, (PRPP); phosphoribosylaminoimidazolesuccinocarboxamide, (SAICAR); plus adenine crADSL to plus adenine WT comparison, (PP); succinyladenosine monophosphate, (SAMP)

* Corresponding author at: University of Denver, 2155 E. Wesley Avenue Room 543, Denver, CO 80210, USA.
E-mail address: guido.vacano@du.edu (G.N. Vacano).

https://doi.org/10.1016/j.ymgmr.2019.100512
Received 29 June 2019; Received in revised form 23 August 2019; Accepted 24 August 2019

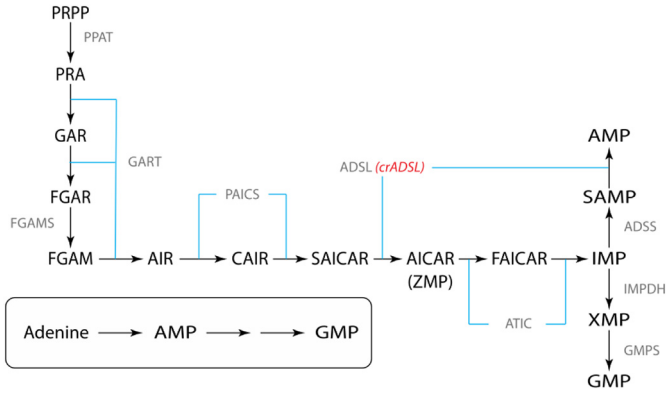

Fig. 1. de novo purine synthetic pathway (DNPS). PRPP is the input small molecule and is converted by six enzymes in ten steps to IMP and is further processed to either AMP or GMP via two additional steps. ADSL is responsible for SAICAR to AICAR and SAMP to AMP. crADSL is the CRISPR generated HeLa cell line used in this study that lacks ADSL enzyme.

within the cell including energy production/regulation via ATP, GTP, and cAMP, cellular signaling, growth, and regulation of other pathways. Recently, the intermediate SAICAR was found to allosterically bind pyruvate kinase M isoform 2 (PKM2) [5], the dominant isoform present in tumors. PKM2 catalyzes the last and only irreversible step of glycolysis, forming pyruvate from phosphoenol pyruvate. The dominance of this isoform in tumors is thought to be the root of the Warburg Effect: the production of lactic acid and consequent metabolic reprogramming via aerobic glycolysis in tumor cells [6]. PKM2 was also found to act as a co-regulator of transcription [7] by binding transcription factors. SAICAR binding to PKM2 is thought to activate a "moonlighting" PKM2 protein kinase activity that acts to directly alter transcription [7]. However, this hypothesis is controversial [8]. SAICAR was also shown to bind both the dimeric and tetrameric forms of PKM2 [9] although recent work suggests that the binding of SAICAR to the dimer promotes its pyruvate kinase activity [9]. PKM2 was found to induce the hypoxia inducible factor 1 subunit alpha (HIF1α) protein upon nuclear translocation of PKM2 [10] which initiates angiogenic and tumorigenic-related events in the cell. SAICAR also accumulates in glucose starved conditions [7] although the mechanism for this is not well understood.

Recently, CRISPR-Cas9 was used to generate knock-outs of the enzymes involved in DNPS including ADSL (designated crADSL) [11]. The crADSL cells have approximately 1.7% ADSL activity compared to wild type cells [11], accumulate SAICAR [12] and fail to grow in the absence of adenine [11]. To investigate the utility of crADSL as a model for ADSL deficiency, RNA-seq was employed to determine transcriptome differences between crADSL and wild type HeLa (WT) cells cultured for 10 h in the presence/absence of adenine. RNA-seq is a tool that can provide a snapshot of global transcriptional activity and can aid in characterizing cellular response to mutations, nutrients, stressors, etc. Changes in gene transcription can be rapidly identified and parsed into various groupings, such as gene ontologies or characterized pathways and reactions. As an initial step in understanding alterations in gene expression in ADSL deficiency, we used RNA-seq to compare gene expression in wt HeLa and crADSL cells in the presence and absence of SAICAR accumulation.

2. Materials and methods

2.1. Cell culture

crADSL was constructed as described previously [11]. HeLa cells (CCL-2) were purchased from ATCC (Manassass, Virginia, USA). Cells were grown on 60 mm TPP plates (Techno Plastic Products, AG, Switzerland) with regularly refreshed Dulbecco's Modified Eagle Medium (DMEM, Gibco) supplemented with 10% fetal calf serum (FCS), 30 μM adenine, and normocin (Invivogen). For purine deprivation experiments (hereafter referred to as starvation), complete medium with 30 μM adenine was exchanged two days and one day before starvation. Adenine is used as a nutritional supplement for DNPS experiments as it can be converted to AMP and GMP via enzymes not affected by DNPS knockouts [13]. Ten to twelve hours prior to starvation, medium was exchanged to DMEM 10% FCS with 100 μM adenine, a concentration of adenine that completely inhibits DNPS [14]. To induce starvation or control conditions, once plates reached ~50–70% confluence, medium was changed to DMEM supplemented with 10% FCM (fetal calf macroserum is FCS dialyzed against saline using a 3.5 kDa barrier), normocin, with or without 100 μM adenine. For cell colony staining experiments, cells were plated in complete growth medium and then medium was exchanged for DMEM 10% FCM, normocin, with or without 30 μM adenine. Cells were fixed in 10% ethanol/3.5% acetic acid solution then stained using 0.1% crystal violet solution.

2.2. HPLC analysis of SAICAR metabolite accumulation

At each time point, cell culture medium was aspirated and cells were washed once with 1 ml cold (4 °C) 1× PBS and then extracted with 500 μl cold (−20 °C) 80% EtOH. Plates were then thoroughly scraped and the cell material was transferred to microfuge tubes and centrifuged at 14,000 ×*g* for 15 min at 4 °C. The supernatant was collected and stored at −80 °C. Samples were dried using a Speedvac, then resuspended in 300 μl freshly prepared mobile phase (50 mM lithium acetate, 5 mM tetra butyl ammonium phosphate, 2% acetonitrile, pH 4.1). Cellular debris was pelleted by two rounds of centrifugation at 14,000 ×*g* for 20 min. Supernatant was frozen at −20 °C until analysis. Samples were transferred to HPLC vials and loaded in an autosampler kept at 10 °C over the course of the runs. Separation of SAICAR was achieved by HPLC–EC analysis similar to our previously described method [15]. Briefly, separation was obtained using reverse phase HPLC–EC with a TSKgel ODS-80Tm C-18 column (250 mm × 4.6 mm ID, 5 μM) protected by Tosoh Bioscience TSKgel guard cartridge. A column temperature of 33 °C was maintained throughout the analysis. Mobile phase was delivered at a flow rate of 0.7 ml/min. Sample extracts and standards were kept at 10 °C and a 30 μl aliquot of each sample was injected using an ESA autosampler (model 542) using a 30 μl partial loop. After injection and separation, analytes were detected using a CoulArray HPLC system (model 5600A, ESA) with three electrochemical detector modules (four flow-through coulometric detectors in series per module for a total of twelve detectors). EC channels were set to a range of potentials from 0 to 900 mV in 100 mV increments, then 1200 mV and 0 mV. Autosampler temperature was kept at 10 °C over the course of runs. Sum of primary peaks area was used to measure analyte accumulation.

2.3. RNA-seq

Cells were plated on the same day into 60 mm TPP dishes. Four biological replicates were cultured in purine rich or purine free (starvation) media conditions for 10 h as previously described in 2.1, and total RNA was extracted using TRIzol reagent (Sigma) according to the manufacturer's protocol. Final purification was performed via spin columns following the manufacturer's protocol (Machery Nagel), with 50 μl total volume DEPC treated water (Sigma). RNA was quantified by NanoDrop One (Thermo Scientific) and frozen at −80 °C. RNA quality assessment and RNA-seq was performed by The Genomics and Microarray Core Facility at the University of Colorado, Denver. mRNA libraries were constructed using the Nugen Universal Plus mRNA-Seq + UDI kit (cat # 9144–96), and 50 bp single read sequencing was performed employing the Illumina HiSEQ4000. Conversion of .bcl to

FASTQ files was done using CASAVA 2.0.

2.4. Processing

Computation was done on a Dell Precision T1700 computer with an Intel Core i7–4790 3.60 GHz CPU and 32 GB RAM running Linux Mint. The RNA-seq sequences, provided in FASTQ format by the Genomics and Microarray Core Facility at the University of Colorado, Denver, were aligned using hisat2 version 2.1.0 to the "genome_snp_tran" indexed human genome [*H. sapiens*, GRCh38 (ftp://ftp.ccb.jhu.edu/pub/infphilo/hisat2/data/grch38_snp_tran.tar.gz)]. Samtools 1.6 [16] was used to sort entries in the sam file output from hisat2 and convert to bam format. The bam files were processed using the Cufflinks suite version 2.2.1 [17] with the "advanced" Cufflinks workflow: Cufflinks → Cuffmerge → Cuffquant → Cuffdiff. The Cuffdiff output was processed using CummeRbund 2.24.0 [18] and various R and bash scripts (described or provided in Supplemental Material). For each mutant vs. WT comparison, the gene_exp.diff file was filtered for significant entries where FPKM values were FPKM ≥ 1 and log2 fold change values were log2 ≥ 1 or log2 ≤ -1 (i.e., 2-fold or greater). The 100 DEGs with the highest absolute log2 values (positive and negative) were combined to generate lists of 200 genes for subsequent ClueGO analyses. Comparisons of crADSL to WT in conditions lacking adenine (MM, or "minus to minus" comparison) and in adenine supplemented conditions (PP, or "plus to plus" comparison) were performed.

2.5. ClueGO analysis

ClueGO is a Cytoscape app that extracts representative functional biological information for large lists of genes or proteins [19]. ClueGO analyses were performed using Cytoscape version 3.7.0 and ClueGO 2.5.2. The GO and Reactome releases were Homo Sapiens_GO-EBI-UniProt-GOA_17.12.2018 and Homo Sapiens_REACTOME_17.12.2018. Data sets were run pairwise using the crADSL plus adenine vs. WT plus adenine comparison (PP) and the crADSL minus adenine vs. WT minus adenine comparison (MM) with the DEG lists described above. Analyses were performed using default settings: the evidence code was set to "all", and network specificity was set to "representative" with a 3 gene/term cut off, approximating GO levels 3–11. Terms and groups were divided into three categories (MM, PP, or Shared) based on whether most genes defining a term or group were enriched in the MM or PP comparisons, or an equal number of significant genes was obtained from both groups (Shared). Further, "slightly enriched" denotes enrichment by one gene, while "heavily enriched" denotes enrichment by two or more genes.

2.6. BiNGO analysis

BiNGO 3.0.3 is a Cytoscape app that analyzes a total gene list and performs GO term enrichment (Biological Process, Cellular Component, and Molecular Function) [20]. Gene lists were analyzed, and ontologies evaluated by False Discovery Rate (FDR). Nodes are colored according to their associated *p*-value.

2.7. qPCR validation of DEGs

qPCR was performed to validate the reliability of the RNA-seq analysis. Total RNA was prepared as described above and concentrations obtained by NanoDrop (ThermoFisher). cDNA was prepared using iScript cDNA synthesis kit (BioRad #1708890) using 500 ng total RNA per reaction according to the manufacturer's protocol. Candidate genes were selected and primers ordered from IDT using PrimeTime service. The primers are TGFβI (Hs.PT.58.40018323), ALPP (Hs.PT.56a.38602874.g), Twist1 (Hs.PT.58.18940950), IQGAP2 (Hs.PT.58.28018594), GATA3 (Hs.PT.58.19431110), β-Actin (Hs.PT.39a.22214847), OASL (Hs.PT.58.50426392), TUSC3 (Hs.PT.58.3740957), and DPYSL3 (Hs.PT.58.39796068). qPCR was performed on IQ5 (BioRad) with 1 µl of cDNA using IQ Sybr Green Supermix (BioRad #170–8880) and the program: 95 °C for 5 min followed by 45 cycles of 95 °C for 10 s and 60 °C elongation. Samples were read 30 s. C_t values were obtained, normalized to β-Actin, and used for further analysis.

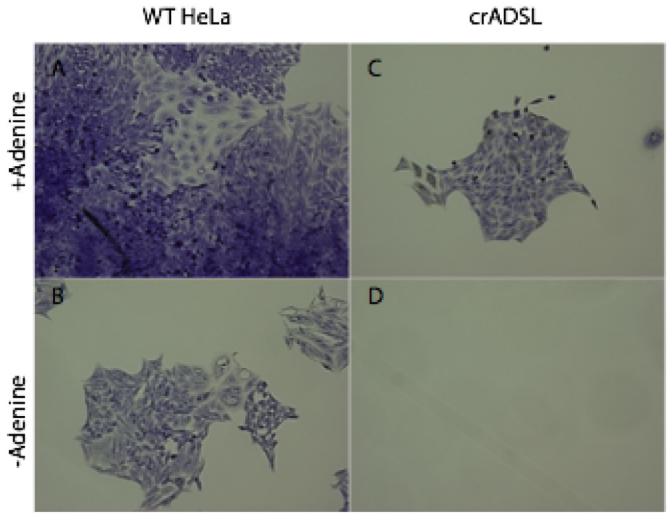

Fig. 2. Adenine is required for proliferative growth of crADSL line. WT HeLa cells (A, B) and crADSL HeLa (C, D) were in DMEM supplemented with 10% FCM with (A, C) or without (B, D) 100 µM adenine then fixed and stained with crystal violet. (For interpretation of the references to colour in this figure legend, the reader is referred to the web version of this article.)

3. Results

3.1. crADSL requires adenine for proliferative growth

Cell growth and purine requirement were assessed for crADSL and WT HeLa cells. When starved long term for purines, crADSL cells showed detachment from the plate and cell death in adenine depleted (purine free) media. In adenine supplemented media, we observed that crADSL takes more time to attach after re-plating and grows more slowly than WT HeLa. WT HeLa showed proliferative growth in both adenine-supplemented and non-supplemented media (Fig. 2). These results confirm a requirement for purine supplementation for crADSL for proliferative growth.

3.2. SAICAR accumulates in crADSL but not WT HeLa cells

HPLC-EC analysis of metabolites from starved crADSL and WT cells was performed to characterize SAICAR accumulation (Fig. 3). In crADSL, the ADSL substrate SAICAR eluted at 50.1 min (Supplemental Fig. 1) with detectable accumulation at 6 h in starvation medium, but not in adenine supplemented medium, and continued until 10 h, the last time point measured. The ADSL product AICAR, which elutes at 24 min, was not observed and SAMP, the second substrate of ADSL, was not observed. This result is consistent with the DNPS pathway block due to ADSL inactivation.

3.3. crADSL and WT show DEGs in both adenine rich and depleted conditions

In the experiments described below, purine deprived cells are labeled M and cells in supplemented medium are labeled P. RNA-seq analysis was performed to detect transcriptome changes by cell type and adenine supplementation. Entries with FPKM (fragments per kilobase of exon per million reads mapped) values < 1 were dropped

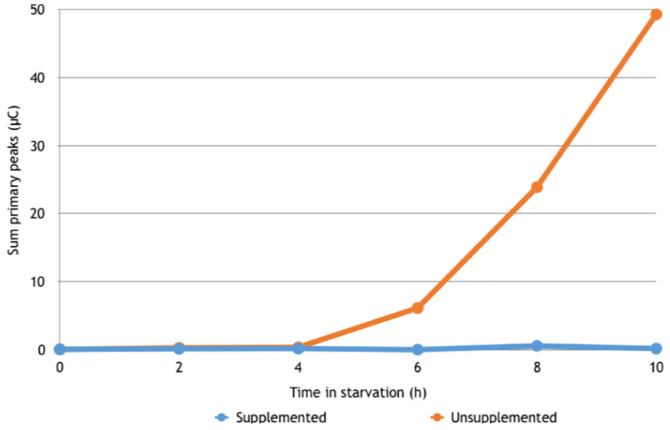

Fig. 3. SAICAR accumulates in crADSL cells in starvation conditions without adenine. crADSL cells were cultured in 100 μM adenine supplemented (blue) or adenine-free (orange) DMEM with 10% FCM for 10 h. Metabolites were analyzed on HPLC-EC. The plot indicates the sum of the primary peaks. (For interpretation of the references to colour in this figure legend, the reader is referred to the web version of this article.)

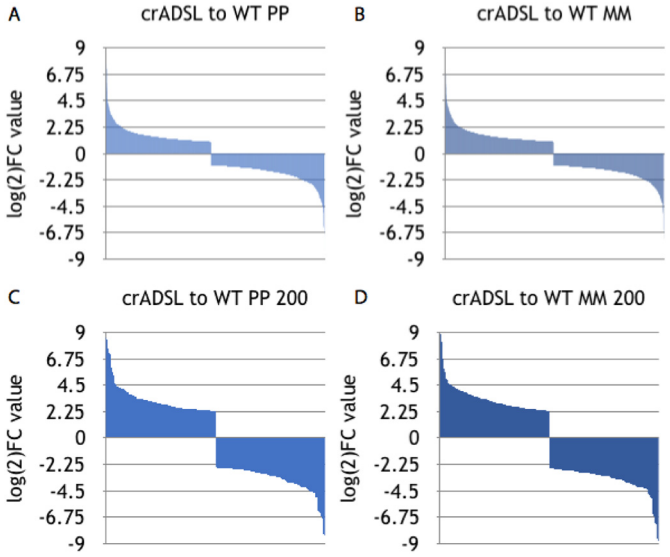

Fig. 4. log(2) fold change of DEGs in cell lines under experimental conditions. A and B: all DEGs that satisfy cutoff constraints between PP comparison (A) and MM comparison (B). C and D: 100 most positively and 100 most negatively changed DEGs in PP comparison (C) and MM comparison (D).

Table 1
Shared and unique DEGs between comparison groups. Total gene counts that satisfied previously defined cutoffs in total gene list in top 200 genes that were used for ClueGO analysis parsed into the PP and MM comparisons or shared between the two comparison groups.

	Total significant DEGs	Top 200 DEGs
Shared	1144	153
Unique PP	282	47
Unique MM	515	47

(which removes low count statistical anomalies), and only ≥2-fold FPKM changes (log2 ≥ 1 or log2 ≤ −1) were retained with a *p*-value cut off of 0.05 using Benjamini-Hochberg correction in Cufflinks [17]. Comparison of crADSL to WT in conditions lacking adenine (MM, or "minus to minus" comparison) returns 1659 DEGs (Supplemental Tables 1, 2). A list of the 100 most positive and 100 most negative DEG log2 values was prepared and encompasses log2 value ranges of 8.823 to 2.311 and −2.593 to −8.788, respectively. Comparison of crADSL to WT in adenine supplemented conditions (PP, or "plus to plus" comparison) returns 1426 DEGs. A list of 100 most positive and 100 most negative DEG log2 values was prepared and encompasses log2 value ranges of 8.577 to 2.266 and −2.526 to −8.289, respectively (Fig. 4). For our generated full list of DEGs, there were 1144 shared genes and 282 (19.8%) and 515 (31.6%) unique identified genes respectively from the PP and MM comparisons. When the list was reduced to the top 200 DEGs used for further analysis, 153 genes were shared between the two comparison groups and 47 unique genes for each PP and MM comparison (Table 1, Supplemental Table 1). Our analysis was limited to genes from the lists derived from each MM and PP comparison.

3.4. crADSL and WT HeLa DEGs: Enrichment in ontology terms and groupings in supplemented and starvation conditions

Gene Ontologies (GO) are divided into three categories: biological process, cellular component, and molecular function. Each category has a specific aim: biological process includes genes that contribute to completion of a biological objective, cellular component refers to gene product localization, and molecular function refers to the biochemical activity of gene products [21]. The Reactome knowledgebase systematically maps gene products into pathway and reaction networks (or metabolic maps, [22]). In our discussion of ontology and Reactome enrichment in the gene sets, term will be used for a singular ontology or Reactome annotation that shows enrichment due to genes associated with that specific component, pathway, process, reaction, or function. It is important to note that terms may be enriched in a single comparison; that however does not indicate that the term was not significant in the other comparison.

In GO Biological Process, DEGs mapped to 95 shared terms in 27 groups (See Fig. 5, for details see Supplemental Table 2 and Supplemental Figs. 2 and 3) The most notable among these are epithelial to mesenchymal transition with 29.65% of terms related to this group, amyloid fibril formation with 12.06% of terms associated, and actin nucleation at 7.04%. Other notable shared terms involve processes such as smooth muscle cell and heart structure development, neuron or brain associated function/development, bone mineralization, hormone processing, as well as interleukins, Wnt signaling, and tumor necrosis factor. In the PP comparisons, we see many overlaps within the shared groupings, however it should be noted that exit from mitosis, and transcription regulatory region DNA binding were heavily enriched terms. For the MM comparisons, we see mass overlap of terms associated with larger parent groups in the shared list, however Glycosaminoglycan catabolic process as well as some actin/myosin-based terms were heavily enriched while terms associated with TGFβ were mildly enriched.

The Cellular Component ontology produced 6 shared terms in 4 groups (Supplemental Table 2, Supplemental Figs. 4, 5). Extracellular matrix, platelet alpha granule, as well as peroxisomal membrane were shared. Mild enrichment was noted in the PP comparison lamellipodium membrane and filopodium, while for the MM comparison with 4 terms in 4 groups centered around plasma membrane, golgi, and photoreceptors.

Molecular Function ontology showed 9 shared terms in 8 groups (Supplemental Table 2, Supplemental Figs. 6, 7) in RNA binding at 22.22%, integrin binding at 11.11% Cell-cell adhesion, Laminin binding, and protein self-association type groupings. Mild enrichment in the PP showed 3 terms in 3 groups in Histone acetyltransferase activity, HMG box domain binding, and R-SMAD binding activity while MM has term enrichment in Aβ and TGFβ binding and lipoprotein particle receptor binding.

The Reactome Pathway results showed 10 shared terms in 4 groups (Supplemental Table 2, Supplemental Figs. 8, 9) involved with kinase activity as well as antiviral mechanism by IFN-stimulated genes at

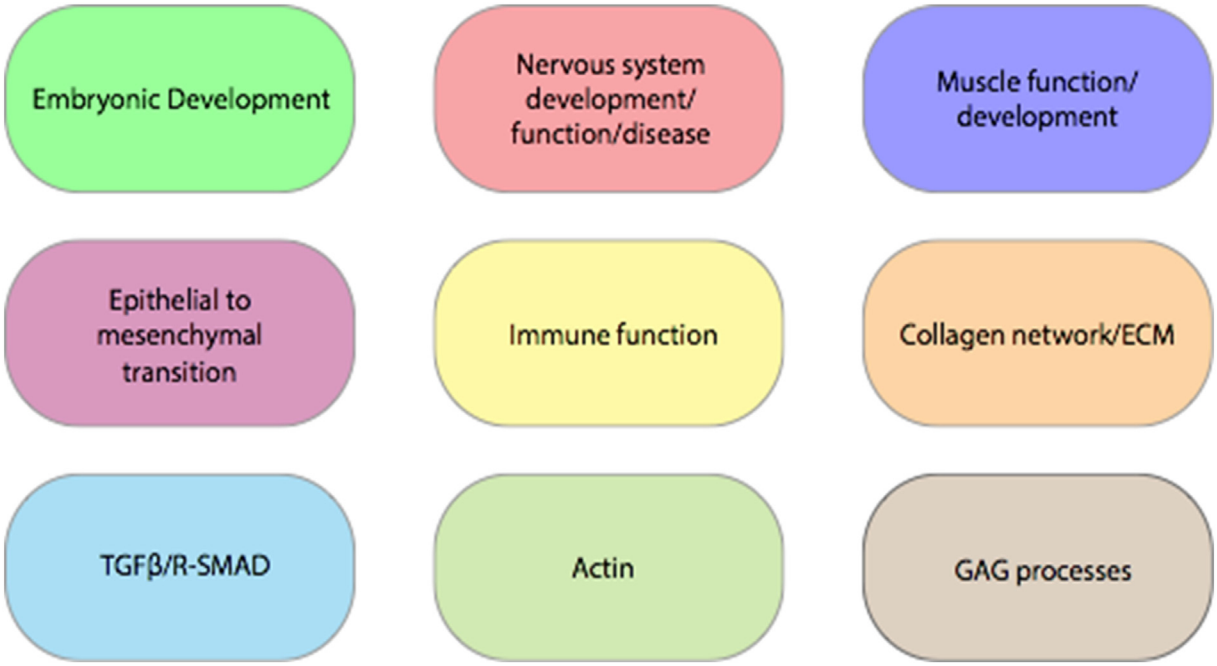

Fig. 5. Notable processes identified via ClueGO analysis.

7.41% gene term association term and complement cascades. Collagen type terms were also strongly enriched in shared pairings due to COL15A1, COL25A1, COL3A1, and COL4A4 being present in both lists analyzed. There were no strong preferential associations in the PP list with 5 terms in 4 groups, however slight enrichment in the PP terms were seen in scavenger receptor ligands, EPH-ephrin repulsion, and signaling by PDGF. Immune system terms OAS antiviral response and IFNG response (with 33.33% and 5.43% gene term association respectively) were seen in the PP comparison. The MM comparison showed more interesting enrichment with 19 terms in 6 groups. Due to the TMOD1 and TNNT1 gene differential expression, striated muscle contraction was heavily enriched. HS-GAG metabolism and other terms associated with GAG were heavily enriched in the MM comparison due to differential expression of GPC5 and HSPG2. For genes slightly enriched in the MM comparison over the PP comparison, collagen related terms such as integrin, ECM proteoglycans, and NCAM, CRMPs and semaphorin, as well as post-translational modification were also slightly enriched in the MM comparison. Various interferon and antiviral terms were slightly enriched in the MM comparison.

The Reactome Reactions results showed similar patterns as Pathways, with strong enrichment in the MM comparison over the PP comparison. Twenty terms in three groups were shared (Supplemental Table 2, Supplemental Figs. 10, 11) and centered around collagen with 90.0% term enrichment, granule membrane proteins, and platelet alpha granule with 5.0% each. The singular enriched PP term associated with IFNG was only slightly enriched. MM comparison revealed 17 terms in 6 groups. Heavily enriched terms in the MM comparison were associated with muscle contraction due to the TMOD1 and TNNT1 gene. GAG based tetrasaccharide linker terms were heavily enriched due to the presence of GPC5 and HSPG2. For terms that were slightly enriched in the MM comparison, we see once again interferon and immune-based terms as well as phosphorylation of CRMPs related terms due to the presence of DPYSL3 (CRMP4) in the MM gene list.

3.5. crADSL and WT HeLa showed similar enrichment patterns using BiNGO analysis

To validate our ClueGO findings, we chose to analyze gene sets using the BiNGO app in Cytoscape. Network maps are shown in Supplemental Table 3 and supplemental Figs. 12–17. While there are new terms that appear in our data sets such as Response to Endoplasmic Reticulum Stress, on the whole this secondary analysis system complements our ClueGO findings.

3.6. Validation of gene expression patterns by qRT-PCR

Candidate gene transcripts were selected that showed robust expression patterns and qPCR was performed to assess whether the expression pattern was maintained using a different analysis system. Primers for DPYSL3 (CRMP4), Twist1, TUSC3, TGFβI, IQGAP2, GATA3, ALPP, and OASL showed ΔC_t values in similar expression patterns to the RNA-seq data log2 values (Fig. 6), demonstrating the validity of our RNA-seq data set in both P and M conditions (Supplemental Table 4).

4. Discussion

In this study, we evaluated the dietary requirements and metabolite accumulation during purine starvation for crADSL, and we performed RNA-seq to compare the crADSL and WT HeLa transcriptomes in purine supplemented and starved conditions. Further, we performed qPCR to verify our RNA-seq results. Our results demonstrate that crADSL requires purine (adenine) supplementation for proliferative growth, SAICAR accumulates over a time course of ten hours during purine starvation, and we obtain many DEGs both by cell type and adenine supplementation.

Previous results [7] support the hypothesis that SAICAR accumulation should produce robust transcriptome changes via the “moonlighting” PKM2 protein kinase activity. It is important to note that their methods are limited to gene chip experiments and not evaluation of viable cells in culture. We observed changes in both PP and MM (SAICAR accumulating) conditions, which suggests that SAICAR accumulation and general ADSL deficiency both mediate transcriptome alteration. Our results show a greater number of DEGs in the MM versus PP comparison, which suggests that SAICAR may be regulating transcription activity, either by a PKM2-SAICAR co-regulation activity or some other mechanism. If PKM2 does act as a co-regulator of transcription, the PKM2-SAICAR complex may potentially activate a select subset of targets for this activity. Our current experiments suggest a

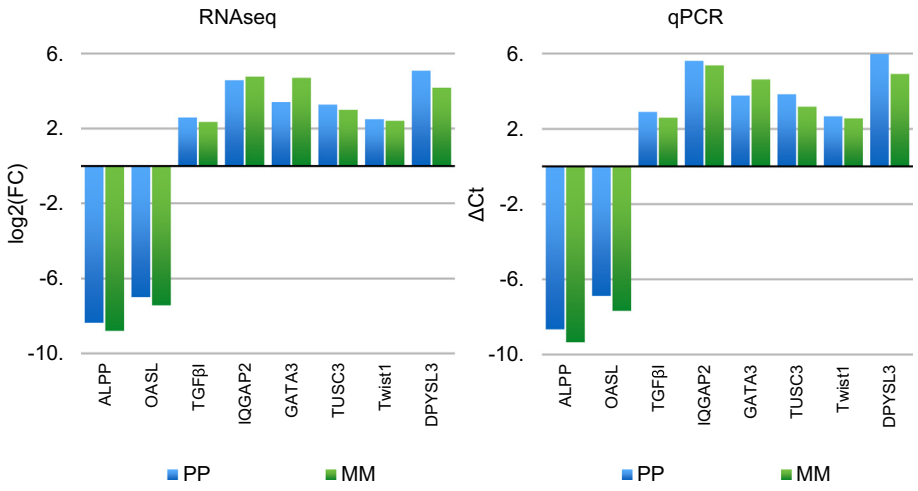

Fig. 6. Candidate gene verification using qPCR. Difference of crADSL against WT cells of biological quadruplicates in both PP and MM of RNAseq (A) and qPCR (B) were normalized to β-Actin. Expression patterns show consistency.

SAICAR derived effect on transcription.

In GO Biological Process, we obtained a robust group of terms including and related to epithelial to mesenchymal transition (EMT) and transforming growth factor beta (TGFβ). EMT refers to the process by which polar epithelial cells undergo biochemical changes that convert them to mesenchymal cells, which exhibit increased resistance to apoptosis and enhanced migratory and invasiveness properties [23]. EMT is important in embryogenesis, specifically during primitive streak formation as well as during neural crest formation. EMT in embryogenesis is orchestrated by the Wnt signaling pathway [23]. Consistent with the EMT related terms, we also observed Wnt signaling pathway in our shared comparison. Disruption in EMT might play an important role in the developmental and neurological phenotypes associated with ADSL deficiency (discussed below). EMT is also important in inflammation and cell migration. Upon trauma to basement membranes, epithelial cells can undergo EMT in response to inflammation from injury [24]. Our results show changes in genes in inflammation/interferon pathways, such as interferon signaling, and IL-1β secretion. Terms associated with interferon, inflammation, and immunity were present in the MM comparison, which suggests that these transcriptional changes are the result of SAICAR accumulation and supports the tentative hypothesis that ADSL deficiency may be an immunological disorder. It also suggests that ADSL deficiency and/or DNPS deficiency may play an important role in immune dysfunction in cancer.

In our GO and Reactome analyses, many shared terms mapped to development associated groups. Since ADSL deficiency is a developmental disorder with phenotypes including dysmorphic features, cognitive deficits, seizures, and psychomotor retardation, it is possible that these terms may be relevant to a plausible explanation of phenotype. In addition, we observed an interesting enrichment in many muscle and movement type terms and groups. This is consistent with the high level of expression of ADSL in muscle cells [25,26] and may be informative to the psychomotor retardation phenotype observed in ADSL deficiency. Our GO and Reactome results indicate that disruption to DNPS (and ADSL specifically) alters energy production and energy levels and sensing needs, which affect force generation in muscle cells.

Cancer is characterized, among other features, by constitutive cellular division, alterations in cellular metabolism (Warburg Effect) [27], collagen network restructuring [28], metastasis and infiltration, and changes in immune function [29,30]. Our results show enrichment for these and related terms, which suggests important roles for DNPS deficiency and/or SAICAR accumulation in these cancer-related processes. In addition to the collagen, integrin, EMT, actin, and ECM terms, our GO cellular component analysis showed enrichment for lamellipodia and filopodia. Filopodia employ integrins to produce finger-like protrusions preparatory to cellular migration. Filopodia formation is an important mechanism for cell migration and infiltration during tumor cell metastasis [31]. Recently, the role of ADSL in certain cancer types was probed suggesting a potential link in aggressive phenotypes [32].

While the scope of this manuscript is focused on the ontologies associated with DNPS and ADSL knockout, several individual genes were identified as of specific interest. Aberrations in ALPP, a placental alkaline phosphatase, have been implicated in spontaneous abortions [33], and in some forms of cancers [34,35]. Twist1 is a transcription factor important for craniofacial and organ development during embryogenesis, most likely from mesoderm derived tissues, and has been identified in multiple types of tumors and involved in cancer metastasis, resistance to chemotherapy, and it can over-ride oncogene induced apoptosis [36]. TUSC3 (tumor suppressor candidate 3) is associated with multiple functions including Mg^{2+} uptake, glycosylation and embryonic development, in addition to its tumor suppression function [37]. IQGAP2 integrates Rho GTPase and Ca^{2+}/calmodulin signals for cellular adhesion and cytoskeleton reorganization and was recently found to act as a tumor suppressor [38]. DPYSL3 (CRMP4) is primarily a neuronal protein expressed during development and adult stages and is responsible for various tasks including cell migration, differentiation, neurite extension, and axonal regeneration [39]. It also has been found to play a role in some non-neuronal cancers in migration and metastasis, although the exact role is still being investigated [40]. GATA3 is a transcription factor and regulator of numerous developmental pathways and has been found heavily associated with breast cancer [41]. OASL is a gene associated with viral response and immunity, with activation carried out by interferons [42]. TGFβI is a ubiquitously secreted ECM protein with plausible participation in morphogenic, embryonic developmental, adhesive/migratory, tumorigenic, wound healing, and inflammatory processes [43]. It is apparent with ontologies and gene variability that DNPS and ADSL provide an important context for the study of developmental and cancer biology.

Individuals with ADSL deficiency have a mutated form of ADSL with reduced enzymatic activity. This implies reduced (but not halted) conversion of SAICAR to AICAR and is consistent with results from patient studies [1,3]. Due to a reduced rate of conversion of SAICAR to AICAR, we would expect transcriptome alteration due to persistent elevation in SAICAR and a reduction in the rate of DNPS. Here we present results detailing transcriptome changes in crADSL due to elimination of ADSL enzyme activity. Future studies will investigate differences between mutant forms of ADSL, and may employ specific cell lines to assess the effects of ADSL dysregulation in developmental,

tumor, vascular and muscle biology. These cells and cells transfected with mutant forms of ADSL should provide an invaluable cellular model of ADSL deficiency.

Funding

This work was funded by The ADSL Research Fund of the Eleanor Roosevelt Institute, The Sam and Frieda Davis TrustSam and Frieda Davis Trust, and The Butler Family Fund of the Denver Foundation.

Declaration of Competimg Interest

The authors have no conflicts of interest.

Acknowledgements

The Cancer Center and the Genomics (Microarray) Shared Resource are supported in part by the Cancer Center Support Grant #P30-CA046934 from the National Cancer Institute.

MZ and VB were supported by Charles University [programmes PRIMUS/17/MED/6 and PROGRES Q26/LF1] and by the Ministry of Education, Youth and Sports of CR [LQ1604 National Sustainability Programme II].

We would like to thank Drs. Anthony Pedley and Hyder Jinnah at Penn State and Emory respectively for their invaluable support and input into this manuscript.

Appendix A. Supplementary data

Supplementary data to this article can be found online at https://doi.org/10.1016/j.ymgmr.2019.100512.

References

[1] A. Jurecka, M. Zikánová, S. Kmoch, A. Tylki-Szymańska, Adenylosuccinate lyase deficiency, J. Inherit. Metab. Dis. 38 (2015) 231–242, https://doi.org/10.1007/s10545-014-9755-y.

[2] T.R. Donti, G. Cappuccio, L. Hubert, J. Neira, P.S. Atwal, M.J. Miller, et al., Diagnosis of adenylosuccinate lyase deficiency by metabolomic profiling in plasma reveals a phenotypic spectrum, Mol. Genet. Metab. Rep. 8 (2016) 61–66, https://doi.org/10.1016/j.ymgmr.2016.07.007.

[3] M. Zikánová, V. Skopova, A. Hnízda, J. Krijt, S. Kmoch, Biochemical and structural analysis of 14 mutant adsl enzyme complexes and correlation to phenotypic heterogeneity of adenylosuccinate lyase deficiency, Hum. Mutat. 31 (2010) 445–455, https://doi.org/10.1002/humu.21212.

[4] G. Caetano-Anollés, L.S. Yafremava, H. Gee, D. Caetano-Anollés, H.S. Kim, J.E. Mittenthal, The origin and evolution of modern metabolism, Int. J. Biochem. Cell Biol. 41 (2009) 285–297, https://doi.org/10.1016/j.biocel.2008.08.022.

[5] K.E.K. Keller, I.S.I. Tan, Y.-S.Y. Lee, SAICAR stimulates pyruvate kinase isoform M2 and promotes cancer cell survival in glucose-limited conditions, Science. 338 (2012) 1069–1072, https://doi.org/10.1126/science.1224409.

[6] W. Yang, Z. Lu, Nuclear PKM2 regulates the Warburg effect, Cell Cycle (Georgetown, Tex). 12 (2013) 3154–3158, https://doi.org/10.4161/cc.26182.

[7] K.E. Keller, Z.M. Doctor, Z.W. Dwyer, Y.-S. Lee, SAICAR induces protein kinase activity of PKM2 that is necessary for sustained proliferative signaling of cancer cells, Mol. Cell 53 (2014) 700–709, https://doi.org/10.1016/j.molcel.2014.02.015.

[8] A.M. Hosios, B.P. Fiske, D.Y. Gui, M.G. Vander Heiden, Lack of evidence for PKM2 protein kinase activity, Mol. Cell 59 (2015) 850–857, https://doi.org/10.1016/j.molcel.2015.07.013.

[9] M. Yan, S. Chakravarthy, J.M. Tokuda, L. Pollack, G.D. Bowman, Y.-S. Lee, Succinyl-5-aminoimidazole-4-carboxamide-1-ribose 5'-phosphate (SAICAR) activates pyruvate kinase isoform M2 (PKM2) in its dimeric form, Biochemistry. 55 (2016) 4731–4736, https://doi.org/10.1021/acs.biochem.6b00658.

[10] W. Luo, H. Hu, R. Chang, J. Zhong, M. Knabel, R. O'Meally, et al., Pyruvate kinase M2 is a PHD3-stimulated coactivator for hypoxia-inducible factor 1, Cell. 145 (2011) 732–744, https://doi.org/10.1016/j.cell.2011.03.054.

[11] V. Baresova, M. Krijt, V. Skopova, O. Souckova, S. Kmoch, M. Zikánová, CRISPR-Cas9 induced mutations along de novo purine synthesis in HeLa cells result in accumulation of individual enzyme substrates and affect purinosome formation, Mol. Genet. Metab. 119 (2016) 270–277, https://doi.org/10.1016/j.ymgme.2016.08.004.

[12] L. Mádrová, M. Krijt, V. Baresova, J. Václavík, D. Friedecký, D. Dobešová, et al., Mass spectrometric analysis of purine de novo biosynthesis intermediates, PLoS ONE 13 (2018) e0208947, , https://doi.org/10.1371/journal.pone.0208947.

[13] M. Kondo, T. Yamaoka, S. Honda, Y. Miwa, R. Katashima, M. Moritani, et al., The rate of cell growth is regulated by purine biosynthesis via ATP production and G(1) to S phase transition, J. Biochem. 128 (2000) 57–64.

[14] A.S. Tu, D. Patterson, Characterization of a guanine-sensitive mutant defective in adenylo-succinate synthetase activity, J. Cell. Physiol. 96 (1978) 123–132, https://doi.org/10.1002/jcp.1040960115.

[15] N. Duval, K. Luhrs, T.G. Wilkinson, V. Baresova, V. Skopova, S. Kmoch, et al., Genetic and metabolomic analysis of AdeD and AdeI mutants of de novo purine biosynthesis: cellular models of de novo purine biosynthesis deficiency disorders, Mol. Genet. Metab. 108 (2013) 178–189, https://doi.org/10.1016/j.ymgme.2013.01.002.

[16] H. Li, B. Handsaker, A. Wysoker, T. Fennell, J. Ruan, N. Homer, et al., The sequence alignment/map format and SAMtools, Bioinformatics. 25 (2009) 2078–2079, https://doi.org/10.1093/bioinformatics/btp352.

[17] C. Trapnell, D.G. Hendrickson, M. Sauvageau, L. Goff, J.L. Rinn, L. Pachter, Differential analysis of gene regulation at transcript resolution with RNA-seq, Nat. Biotechnol. 31 (2013) 46–53, https://doi.org/10.1038/nbt.2450.

[18] L. Goff, C. Trapnell, D. Kelley, cummeRbund: Analysis, Exploration, Manipulation, and Visualization of Cufflinks High-Throughput Sequencing Data, R Package Version, (2019).

[19] B. Mlecnik, J. Galon, G. Bindea, Comprehensive functional analysis of large lists of genes and proteins, J. Proteome 171 (2018) 2–10, https://doi.org/10.1016/j.jprot.2017.03.016.

[20] S. Maere, K. Heymans, M. Kuiper, BiNGO: a Cytoscape plugin to assess over-representation of gene ontology categories in biological networks, Bioinformatics. 21 (2005) 3448–3449, https://doi.org/10.1093/bioinformatics/bti551.

[21] M. Ashburner, C.A. Ball, J.A. Blake, D. Botstein, H. Butler, J.M. Cherry, et al., Gene ontology: tool for the unification of biology. The gene ontology consortium, Nat. Genet. 25 (2000) 25–29, https://doi.org/10.1038/75556.

[22] A. Fabregat, S. Jupe, L. Matthews, K. Sidiropoulos, M. Gillespie, P. Garapati, et al., The Reactome pathway knowledgebase, Nucleic Acids Res. 46 (2018) D649–D655, https://doi.org/10.1093/nar/gkx1132.

[23] R. Kalluri, EMT: when epithelial cells decide to become mesenchymal-like cells, J. Clin. Invest. 119 (2009) 1417–1419, https://doi.org/10.1172/JCI39675.

[24] R. Kalluri, R.A. Weinberg, The basics of epithelial-mesenchymal transition, J. Clin. Invest. 119 (2009) 1420–1428, https://doi.org/10.1172/JCI39104.

[25] G. van den Berghe, J. Jaeken, Adenylosuccinase deficiency, Adv. Exp. Med. Biol. 195 (Pt A) (1986) 27–33, https://doi.org/10.1007/978-1-4684-5104-7_4.

[26] L.M. Brand, J.M. Lowenstein, Effect of diet on adenylosuccinase activity in various organs of rat and chicken, J. Biol. Chem. 253 (1978) 6872–6878.

[27] M.V. Liberti, J.W. Locasale, The Warburg effect: how does it benefit cancer cells? Trends Biochem. Sci. 41 (2016) 211–218, https://doi.org/10.1016/j.tibs.2015.12.001.

[28] M. Fang, J. Yuan, C. Peng, Y. Li, Collagen as a double-edged sword in tumor progression, Tumour Biol. 35 (2014) 2871–2882, https://doi.org/10.1007/s13277-013-1511-7.

[29] L. Iommarini, A. Ghelli, G. Gasparre, A.M. Porcelli, Mitochondrial metabolism and energy sensing in tumor progression, Biochim. Biophys. Acta Bioenerg. 1858 (2017) 582–590, https://doi.org/10.1016/j.bbabio.2017.02.006.

[30] E. Krzywinska, C. Stockmann, Hypoxia, metabolism and immune cell function, Biomedicines. 6 (2018) 56, https://doi.org/10.3390/biomedicines6020056.

[31] A. Arjonen, R. Kaukonen, J. Ivaska, Filopodia and adhesion in cancer cell motility, Cell Adhes. Migr. 5 (2011) 421–430, https://doi.org/10.4161/cam.5.5.17723.

[32] H. Park, K. Ohshima, S. Nojima, S. Tahara, M. Kurashige, Y. Hori, et al., Adenylosuccinate Lyase Enhances Aggressiveness of Endometrial Cancer by Increasing Killer Cell Lectin-Like Receptor C3 Expression by Fumarate, 98 (2018), pp. 449–461, https://doi.org/10.1038/s41374-017-0017-0.

[33] M. Vatin, S. Bouvier, L. Bellazi, X. Montagutelli, P. Laissue, A. Ziyyat, et al., Polymorphisms of human placental alkaline phosphatase are associated with in vitro fertilization success and recurrent pregnancy loss, Am. J. Pathol. 184 (2014) 362–368, https://doi.org/10.1016/j.ajpath.2013.10.024.

[34] W.H. Fishman, Clinical and biological significance of an isozyme tumor marker–PLAP, Clin. Biochem. 20 (1987) 387–392.

[35] W.H. FISHMAN, N.R. INGLIS, S. GREEN, C.L. ANSTISS, N.K. GOSH, A.E. REIF, et al., Immunology and biochemistry of Regan isoenzyme of alkaline phosphatase in human cancer, Nature. 219 (1968) 697–699, https://doi.org/10.1038/219697a0.

[36] Q. Qin, Y. Xu, T. He, C. Qin, J. Xu, Normal and disease-related biological functions of Twist1 and underlying molecular mechanisms, Cell Res. 22 (2012) 90–106, https://doi.org/10.1038/cr.2011.144.

[37] X. Yu, C. Zhai, Y. Fan, J. Zhang, N. Liang, F. Liu, et al., TUSC3: a novel tumour suppressor gene and its functional implications, J. Cell. Mol. Med. 21 (2017) 1711–1718, https://doi.org/10.1111/jcmm.13128.

[38] Y. Xie, J. Yan, J.-C. Cutz, A.P. Rybak, L. He, F. Wei, et al., IQGAP2, a candidate tumour suppressor of prostate tumorigenesis, Biochim. Biophys. Acta 1822 (2012) 875–884, https://doi.org/10.1016/j.bbadis.2012.02.019.

[39] Y.Z. Alabed, M. Pool, S. Ong Tone, A.E. Fournier, Identification of CRMP4 as a convergent regulator of axon outgrowth inhibition, J. Neurosci. 27 (2007) 1702–1711, https://doi.org/10.1523/JNEUROSCI.5055-06.2007.

[40] R. Matsunuma, D.W. Chan, B.-J. Kim, P. Singh, A. Han, A.B. Saltzman, et al., DPYSL3 modulates mitosis, migration, and epithelial-to-mesenchymal transition in claudin-low breast cancer, Proc. Natl. Acad. Sci. 115 (2018) E11978–E11987, , https://doi.org/10.1073/pnas.1810598115.

[41] J. Chou, S. Provot, Z. Werb, GATA3 in development and cancer differentiation: cells GATA have it!, J. Cell. Physiol. 222 (2010) 42–49, https://doi.org/10.1002/jcp.21943.

[42] U.Y. Choi, J.-S. Kang, Y.S. Hwang, Y.-J. Kim, Oligoadenylate synthase-like (OASL) proteins: dual functions and associations with diseases, Exp. Mol. Med. 47 (2015), https://doi.org/10.1038/emm.2014.110 e144–e144.

[43] N. Thapa, B.-H. Lee, I.-S. Kim, TGFBIp/betaig-h3 protein: a versatile matrix molecule induced by TGF-beta, Int. J. Biochem. Cell Biol. 39 (2007) 2183–2194, https://doi.org/10.1016/j.biocel.2007.06.004.